



**HAL**  
open science

## Ramping up RF power and increasing pulse length in the full tungsten environment of WEST

C. Bourdelle, J. Bucalossi, N. Fedorczak, T. Loarer, E. Moreau, J.-F Tsitrone, V Artaud, S. Brezinsek, H. Bufferand, L. Colas, et al.

► **To cite this version:**

C. Bourdelle, J. Bucalossi, N. Fedorczak, T. Loarer, E. Moreau, et al.. Ramping up RF power and increasing pulse length in the full tungsten environment of WEST. 46th EPS Conference on Plasma Physics, Jul 2019, Milan, Italy. hal-02395304

**HAL Id: hal-02395304**

**<https://hal.science/hal-02395304>**

Submitted on 5 Dec 2019

**HAL** is a multi-disciplinary open access archive for the deposit and dissemination of scientific research documents, whether they are published or not. The documents may come from teaching and research institutions in France or abroad, or from public or private research centers.

L'archive ouverte pluridisciplinaire **HAL**, est destinée au dépôt et à la diffusion de documents scientifiques de niveau recherche, publiés ou non, émanant des établissements d'enseignement et de recherche français ou étrangers, des laboratoires publics ou privés.

## Ramping up RF power and increasing pulse length in the full tungsten environment of WEST

C. Bourdelle, J. Bucalossi, N. Fedorczak, T. Loarer, Ph. Moreau, E. Tsitrone, J.-F. Artaud, V. Bobkov<sup>1</sup>, S. Brezinsek<sup>2</sup>, H. Bufferand, L. Colas, Y. Corre, X. Courtois, L. Delpech, C. Desgranges, P. Devynck, T Dittmar<sup>2</sup>, A Drenik<sup>1</sup>, D. Douai, R. Dumont, F. Durodié<sup>3</sup>, A. Ekedahl, J. Garcia, J. Gaspar<sup>4</sup>, C. Gil, M. Goniche, J. Gunn, W. Helou<sup>5</sup>, J. Hillairet, P. Hennequin<sup>6</sup>, C.C. Klepper<sup>7</sup>, E. Lerche<sup>3</sup>, P. Maget, Y. Marandet<sup>8</sup>, D. Mazon, O. Meyer, G. Lombard, P. Manas, P. Mollard, J. Morales, E. Nardon, R. Nouailletas, M. Peret, Y. Peysson, C. Reux, F. Saint-Laurent, J.-L. Schwob<sup>9</sup>, P. Tamain, G. Urbanczyk, S. Vartanian, L. Vermare<sup>6</sup>, D. Vézinet, X. Yang<sup>10</sup> and the WEST team\*

CEA, IRFM, F-13108 Saint Paul-lez-Durance, France

<sup>1</sup> Max-Planck -Institut für Plasmaphysik, 85748 Garching b. München, Germany

<sup>2</sup> Forschungszentrum Jülich, IEK, TEC, 52425 Jülich, Germany

<sup>3</sup> LPP-ERM/KMS - BE-1000 Brussels-Belgium

<sup>4</sup> Aix-Marseille Université Laboratoire IUSTI

<sup>5</sup> ITER Organization, Route de Vinon-sur Verdon, 13067 St. Paul Lez Durance, France

<sup>6</sup> Ecole Polytechnique, LPP, CNRS UMR 7648, 91128

<sup>7</sup> Oak Ridge National Laboratory, Oak Ridge, TN 37831-6169, USA

<sup>8</sup> PIIM, CNRS-Université de Provence, Marseille, France

<sup>9</sup> Racah Institute of Physics, The Hebrew University, IL-91904 Jerusalem, Israel

<sup>10</sup> University of Science and Technology of China, Hefei, People's Republic of China

\* <http://west.cea.fr/WESTteam>

**Introduction.** WEST is a full tungsten (W) superconducting actively cooled tokamak with a plasma volume of 14 m<sup>3</sup>, a major radius of 2.5 m, an aspect ratio A between 5 and 6 and a magnetic field of 3.7T. WEST programme aims at power/particle exhaust studies on the ITER-like actively cooled tungsten divertor and at bulk plasma performance in discharges reaching 1000s [1,2]. It is equipped with 9 MW of ICRH power and 7 MW of LHCD.

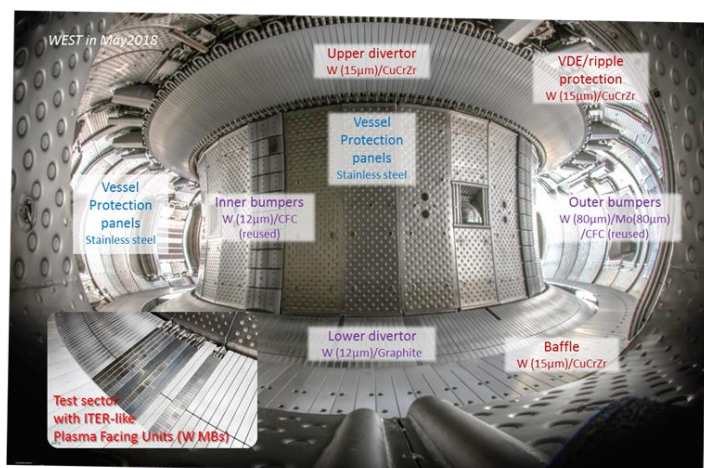


Figure 1: picture of WEST vacuum vessel, May 2018.

After an integrated commissioning phase (Dec.2016 – Dec. 2017) [4,5], diverted plasmas became routinely available. In 2018, 20 weeks of operation allowed to ramp up the RF power

The upper divertor is made of actively cooled W coated copper tiles. In the present phase 1 of WEST, the lower divertor is equipped with a set of actively cooled ITER-like units, complemented with inertially cooled W coated units. Other side limiters are all W coated, figure 1.

reaching 5.3 MW with LHCD [7] and 1.4 MW with the 2 new ICRH antennas [6]. The main plasma configuration was in Lower Single Null, but we also operated in Double Null as well as in Upper Single Null, in particular to perform long pulses on the actively cooled upper divertor. Thanks to reproducible 30s pulses, 20 minutes of plasmas were achieved in 2 days in USN at the end of the 2018 operation. Up to 0.8 MA plasmas were obtained. Thanks to 3 boronisations [8], the operational window opened up to higher density range. Nonetheless, the fraction of radiated power remained around 50% of the LHCD power [9] and up to 100% in some cases for ICRH power [10]. This radiated fraction prevented to achieve H mode so far, despite a sheared radial electric field. A complex interplay between W and core (2,1) MHD modes [11] (see figure 2 just after 6 s for example) required scenario adjustments in terms of  $I_p$  and LHCD ramp up. This paper presents the first analysis performed for high performance discharges: study of confinement for a high power shot and tungsten transport for a long pulse. First, the confinement of a 5MW pulse at  $A=5.6$  is discussed with respect to the existing scaling laws. Then a 33s electron heated, low torque plasma is presented. Throughout the pulse, the W concentration remains stable around  $3 \times 10^{-4}$ , and, consistently, the modelled W peaking is found twice lower than the measured electron density peaking.

### **Ramping up the RF power. Aspect ratio impact on scaling laws.**

Time traces of a typical high power pulse are displayed on figure 2. The fraction of radiated power is 50%. A resistive  $Z_{\text{eff}}$  of 2.1 is estimated during the ohmic flat top phase thanks to  $T_e$  from ECE and the measured flux consumption. The ECE central electron temperature reaches 5 keV at  $\bar{n} = 3.5 \times 10^{19} \text{ m}^{-3}$ , i.e. 55% of the Greenwald density. The Doppler reflectometry measures a sheared radial electric field at the plasma periphery. Despite this, H mode is not achieved. The power crossing the separatrix (2.8 MW at 8s) is still below the scaling laws [12,13], see figure 3.a. The confinement time (at 8s) is estimated using the energy content from the equilibrium reconstruction [14] and the total injected power (without subtracting the bulk  $P_{\text{rad}}$ ). It is compared to  $\tau_E$  predicted by H98P(y,2), leading to an H factor of 0.8. The meaning of this factor is highly questionable as illustrated by figure 3.b where by changing the aspect ratio from 5.6 to 3, the H factor varies from 0.8 down to 0.55, while the distance to the L mode prediction stays identical. Including WEST data in the international database (note that WEST data are in the IMAS format [15]) as well as using 1<sup>st</sup> principles modelling will contribute to revisit the impact of A on confinement,.

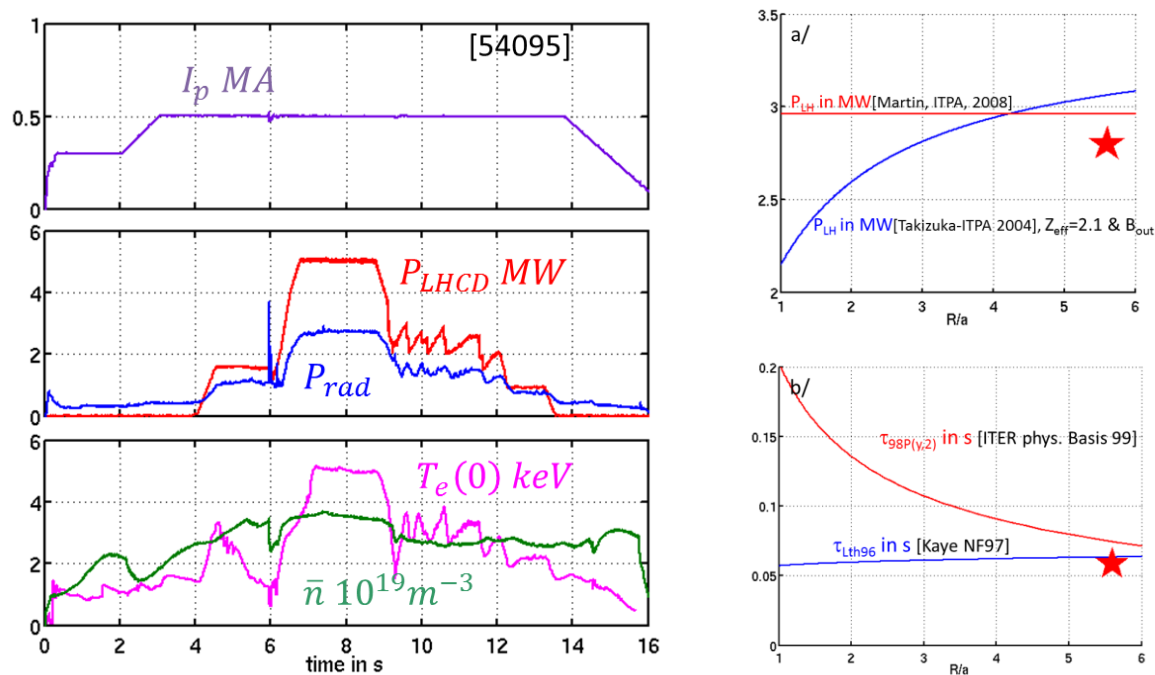


Figure 2 (left): Time traces for WEST pulse 54095.

Figures 3 (right): a/ L to H power threshold scaling laws [12,13] versus  $A=R/a$ . The red star corresponds to the power crossing the separatrix for 54095 at 8s b/ the H98P(y,2) and Lth96 predicted confinement times are plotted versus  $A$ , using the parameters from 54095 at 8s. The red star corresponds to the confinement time of 54095 at 8s at  $A=5.6$ .

### W transport in 30 s L modes

In dominant electron heated plasmas, in absence of torque, it is of high interest to observe and understand the W behavior. The time trace of 54178 (figure 4) shows that the density is well controlled and that the bulk radiated power remains stable during the LHCD only heated phase (the SXR peaking as well as visible WI lines are also stable throughout this pulse see [16]). During the ICRH phase, 100% of the 0.6 MW of ICRH are radiated (figure 4) and the central electron temperature slightly decreases, for a more detailed analysis of the plasma response to ICRH see [10]. During N<sub>2</sub> seeding, an increase of both the neutron rate (see [16]) and  $T_e(0)$  is measured, figure 4. A first systematic estimate of the W concentration is inferred from the total bulk radiative power measured by bolometry to which the contribution from low Z impurities (assuming N only contributes to  $Z_{\text{eff}}$ ) is subtracted assuming that W is the only metallic impurity and that all impurity profiles are homothetic to  $n_e$ . This serves as the starting point for more refined iterations between 1.5D integrated modelling by METIS [17] and the SXR, bolometer, Bremsstrahlung synthetic reconstruction of all the line of sights using TOFU [18].

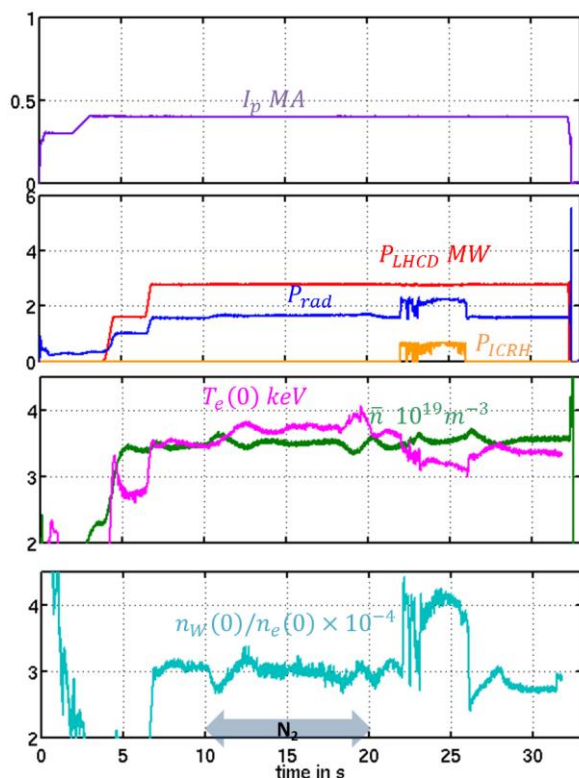


Figure 4: time traces of 54178.

Thanks to a microstability analysis performed with the qualinear gyrokinetic code QuaLiKiz [19] for turbulent transport and the drift-kinetic code NEO [20] for neoclassical transport, it is found that TEM are the dominant instabilities in this electron heated pulse (54178 at 8s). The peaked electron density profile at mid-radius ( $R/L_n=5$ ) is due a high  $R/L_n$  threshold for TEM as expected at large A. The W transport is dominated by the turbulent diffusion for  $\rho>0.25$ , figure 5, leading to a W density peaking twice lower than the electron density peaking. Inside  $\rho<0.25$ , the W peaking is determined by neoclassical transport. Note that an artificially increased toroidal rotation up to 100km/s results in a factor 20 on the core W peaking [16]. Finally, by seeding  $N_2$ , the dilution pushes the ITG threshold to larger  $R/L_{Ti}$ , which could explain the improved confinement [16].

**Conclusions.** First results of WEST allow shedding new light on confinement at high aspect ratio and tungsten transport in electron heated/low torque plasmas of interest for ITER. The coming 2019 campaign will be targeted at further increasing RF power (up to 10 MW) and pulse length (up to 1 mn), and performing a He campaign. Phase 2 will start in spring 2020 with a complete ITER-like lower divertor [3], aiming at 1000s H modes, more on [our portal](#).

[1] J. Bucalossi, FED (2014) [2] C. Bourdelle, NF (2015) [3] J. Bucalossi, SOFE (2019) [4] E. Nardon et al EPS (2018) [5] Ph. Moreau et al SOFE (2019) [6] W. Helou RFPPC (2019) [7] L. Delpéch RFPPC (2019) [8] J. Bucalossi PFMC (2019) [9] M. Goniche et al RFPPC (2019) [10] L. Colas et al RFPPC (2019) [12] Y. Martin et al, NF 2008) [13] Takizuka PPCF 2004 [14] B. Faugeras 2017 [15] F Imbeaux et al NF2015 [16] X. Yang et al EPS (2019) [17] JF Artaud NF (2018) [18] D. Vézinet NF (2016) [19] [www.qualikiz.com](http://www.qualikiz.com) Bourdelle (2016) Citrin (2017) [20] E. Belli et al PPCF (2008)

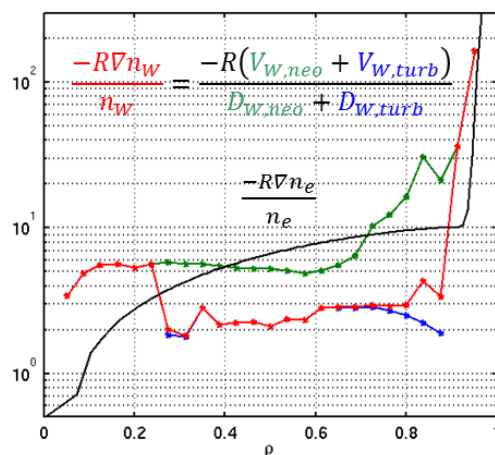


Figure 5:  $\frac{-R\nabla n_W}{n_W}$  of pulse 54178 at 8s. In green the ratio  $\frac{-R\nabla n_{W,neo}}{D_{W,neo}}$  calculated using NEO, in blue  $\frac{-R\nabla n_{W,turb}}{D_{W,turb}}$  calculated by QuaLiKiz, in red  $\frac{-R\nabla n_W}{D_{W,neo}+D_{W,turb}}$ . The electron density peaking is added in black as a reference.